PHYSICAL REVIEW B VOLUME 23, NUMBER 6 15 MARCH 1981

# Many-body Coulomb effects on the gain and absorption line shapes of the electron-hole plasma in GaAs

K. Arya and W. Hanke
*Max-Planck-Institut für Festkörperforschung, 7 Stuttgart-80, Federal Republic of Germany*
(Received 15 October 1980)

Many-body effects due to electron-hole ($e$-$h$) attraction and self-energy corrections are investigated on gain and absorption line shapes of degenerate $e$-$h$ plasma in direct-gap semiconductors. It is demonstrated for GaAs that a large enhancement in experimental gain and absorption coefficients near crossover, which is not reproduced in single-particle treatments, is accounted for by the excitonic $e$-$h$ interaction. The self-energy corrections, containing the renormalization due to $e$-$e$ and $e$-phonon interactions, reduce the direct band gap in GaAs. The fact that the absorption and gain line shapes are sensitive to the plasma density ($n$) and temperature ($T$) in a wide energy range shows that they can be used for determining $n$ and $T$ more accurately than can luminescence studies.

## I. INTRODUCTION

Many-body Coulomb effects play an important role in the optical spectra of semiconductors and insulators. For instance, the absorption line shapes are strongly influenced by the Coulomb interaction between electrons and holes.[1–4] The appearance of bound[1] and unbound[2] excitons near the absorption edge and a large enhancement in the absorption coefficient above the absorption edge which persists for many exciton binding energies in intrinsic semiconductors are a result of this interaction. In doped semiconductors, the electron-hole ($e$-$h$) interaction is screened due to free carriers present in the crystal, thus reducing these effects considerably. However, it is found[3,4] that for carrier concentrations even up to $\sim 10^{18}$ cm$^{-3}$, although one does not see any bound exciton peak, one still finds large enhancements in the absorption line shapes above the absorption edge due to $e$-$h$ interactions. Another important many-body effect in doped crystals is due to the interaction among the free carriers, which is responsible for the reduction of the intrinsic gap[5] and thus for a lowering of the absorption edge.

These many-body effects on the absorption and emission (gain) line shapes have also been studied[6–9] in the case of highly excited semiconductors. In highly excited crystals a large number of free carriers, electrons in the conduction band and holes in the valence band, are created by a separate laser beam and absorption and emission measurements are carried out in the presence of these carriers. In recent experiments on excited crystals,[10,11] for instance, in GaAs, it is found that gain line shapes do not agree well with those obtained from the noninteracting single-particle model. This noninteracting model should reflect the energy square-root behavior for the joint density of states within the parabolic band approximation for the valence and conduction bands. Rather, the experiments show a considerable enhancement in the gain and absorption near the crossover [the crossover from gain to absorption occurs at photon energy $\mu = \mu_e + \mu_h$ where $\mu_e$ ($\mu_h$) is the chemical potential for electrons (holes)].

There have been several attempts[10,11] to fit the experimental gain line shapes by neglecting the momentum ($\vec{k}$-) selection rule for the optical transitions. This is based on the assumption that optical transitions take place mainly due to impurities or defects present in the crystal. However, the impurity concentration is typically three or four orders smaller than the free carrier concentrations. Furthermore, this model completely fails to explain the absorption line shapes far above the absorption edge[12,13] where it results in a diverging ($\omega^2$) behavior for the absorption coefficient.

In this paper, we investigate the many-body effects due to $e$-$h$ attraction and self-energy corrections on the gain and absorption spectra, in particular reference to the $e$-$h$ plasma in GaAs. In Sec. II, we derive an expression for the absorption coefficient including the two many-body effects. The inclusion of $e$-$h$ interaction leads to an integral equation for the two-particle Green's function or interband polarizability which is solved approximately making use of the effective-mass scheme for valence and conduction bands. The self-energy corrections to the single-particle (electron and hole) energies due to Coulomb interaction in the $e$-$h$ plasma are calculated by using a single-plasmon-pole approximation. In Sec. III, we give results for the theoretical line shapes for various values of plasma concentration ($n$) and temperature ($T$). These are discussed in the light of experimental results and are compared with the non-$\vec{k}$-conserving model. One important conclusion that emerges from our studies is that one can in fact

determine accurately the plasma $n$ and $T$ by comparing the theoretical line shapes including many-particle effects with the experimental line shapes.

## II. ABSORPTION AND GAIN COEFFICIENTS INCLUDING MANY-BODY EFFECTS

We calculate here the imaginary part, $\epsilon_2(\vec{q},\omega)$, of the dielectric function which is related to the absorption $[\epsilon_2(\vec{q},\omega)>0]$ and gain $[\epsilon_2(\vec{q},\omega)<0]$ spectrum. The $e$-$h$ interaction is taken into account within the time-dependent Hartree-Fock approximation[2] by including all the ladder diagrams as shown in Figs. 1(b), 1(c), etc., in addition to the noninteracting polarization diagram 1(a). The self-energy corrections are then incorporated by taking the dressed propagators for electrons and holes in these diagrams. This gives

$$\epsilon_2^b(\vec{q},\omega)=\lim_{\delta\to 0}\frac{4\pi e^2}{m^2\omega^2}\,\mathrm{Im}\sum_{\substack{n_1n_2n_3n_4\\ \vec{k},\vec{k}'}}\langle n_2\vec{k}|\vec{p}|n_1\vec{k}+\vec{q}\rangle\chi(n\vec{k}+\vec{q},n_2\vec{k},n_3\vec{k}',n_4\vec{k}'+\vec{q},\omega-i\delta)\langle n_4\vec{k}'+\vec{q}|\vec{p}|n_3\vec{k}'\rangle\ , \tag{1}$$

where the polarization $\chi$ satisfies the integral equation[2]

$$\chi(n_1\vec{k}+\vec{q},n_2\vec{k},n_5\vec{k}'',n_6\vec{k}''+\vec{q},\omega)=\chi^0(n_1\vec{k}+\vec{q},n_2\vec{k},\omega)\Big[\delta_{n_1n_6}\delta_{n_2n_5}\delta_{\vec{k},\vec{k}''}-\frac{1}{2}\sum_{n_3n_4\vec{k}'}v(n_1\vec{k}+\vec{q},n_2\vec{k},n_3\vec{k}',n_4\vec{k}'+\vec{q})\times\chi(n_4\vec{k}+\vec{q},n_3\vec{k}',n_5\vec{k}'',n_6\vec{k}''+\vec{q},\vec{q},\omega)\Big]\ . \tag{2}$$

The zeroth-order polarization $\chi^0$ and the exchange Coulomb interaction $v$ are given as

$$\chi^0(n_1\vec{k}+\vec{q},n_2\vec{k},\omega)=\frac{f_{n_2}(E_{\vec{k}})-f_{n_1}(E_{\vec{k}+\vec{q}})}{E_{n_2}(\vec{k})-E_{n_1}(\vec{k}+\vec{q})+\hbar\omega}\ , \tag{3}$$

$$v(n_1\vec{k}+\vec{q},n_2\vec{k},n_3\vec{k}',n_4\vec{k}'+\vec{q})=(U_{n_1\vec{k}+\vec{q}}(\vec{r})|U_{n_4\vec{k}+\vec{q}}(\vec{r}))(U_{n_3\vec{k}'}(\vec{r})|U_{n_2\vec{k}}(\vec{r}))\,V_s(\vec{k}-\vec{k}')\ , \tag{4}$$

where

$$V_s(\vec{k})=4\pi e^2/(\epsilon_0k^2+k_{\rm FT}^2)\ . \tag{5}$$

In these equations, $n_1,n_2$, etc., denote the band indices, $\vec{p}$ is the momentum operator, $k_{\rm FT}^{-1}$ is the Thomas-Fermi screening length, $\epsilon_0$ is the static dielectric constant, and $f_n(E_{\vec{k}})$ gives the occupation probability for the state with energy $E_n(\vec{k})$. In Eq. (4), $U_{n,\vec{k}}(\vec{r})$ is the periodic part of the Bloch state $\phi_{n\vec{k}}(\vec{r})$ and the integrals are over the unit cell of the crystal.

In Eq. (2), there is a summation over band indices $n_3$ and $n_4$. However, using Eq. (4) we retain terms only for $n_3=n_2$ and $n_4=n_1$, which give maximum contributions. Further in this approximation and in the effective-mass approximation to be used afterwards, for $|\vec{k}-\vec{k}'|\sim k_F$ we take

$$v(n_1\vec{k}+\vec{q},n_2\vec{k},n_3\vec{k}',n_4\vec{k}'+\vec{q})\approx V_s(\vec{k}-\vec{k}')\delta n_1n_4\delta n_2n_3\ . \tag{6}$$

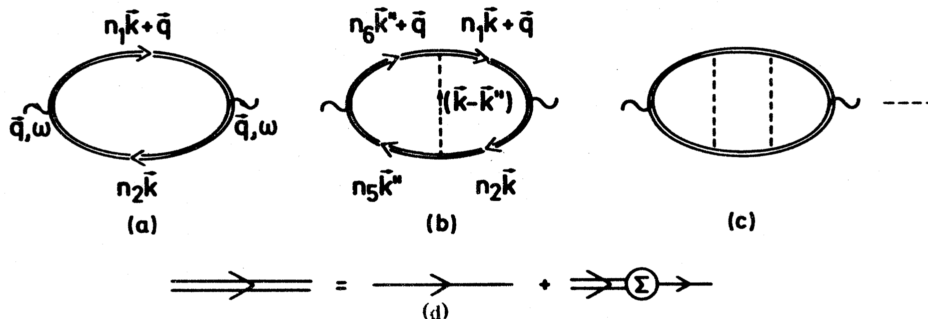


FIG. 1. Ladder diagrams (b,c, etc.) for $e$-$h$ interaction included in the zeroth-order RPA polarization (a). (d) Propagators including self-energy corrections.

As we are interested in the frequency range $\hbar\omega$ close to the energy gap between the conduction and valence bands, Eq. (3) shows that the dominant contributions to $\epsilon_2(\vec{q},\omega)$ come when $n_1$ and $n_2$ correspond to the conduction and valence band, respectively. In GaAs, there are two valence bands, heavy hole ($hh$) and light hole ($lh$) bands both with allowed transitions from the conduction band. However, because of the very small number of holes present in the $lh$ band, the line shapes are mainly determined by transitions between the conduction and $hh$ band and hence we consider only the $hh$ band. Thus Eq. (1) simplifies to

$$\epsilon_2^b(\vec{q},\omega)=\lim_{\delta\to 0} C \sum_{\vec{k},\vec{k}''} \mathrm{Im}\chi_{cv}(\vec{k}+\vec{q},\vec{k}'',\omega-i\delta) \;, \tag{7}$$

where $C=4\pi e^2|P_{cv}|^2/(m^2\omega^2)$ and the integral Eq. (2) for $\chi_{cv}$ becomes

$$\chi_{cv}(\vec{k}+\vec{q},\vec{k}'',\omega)=\chi_{cv}^0(\vec{k}+\vec{q},\vec{k},\omega)\left[\delta_{\vec{k},\vec{k}''}-\frac{1}{2}\sum_{\vec{k}'}V_s(\vec{k}-\vec{k}')\chi_{cv}(\vec{k}'+q,\vec{k}'',\omega)\right] \;, \tag{8}$$

$$\chi_{cv}^0(\vec{k}+\vec{q},\vec{k},\omega)=\frac{f_v(E_{\vec{k}})-f_c(E_{\vec{k}+\vec{q}})}{E_v(\vec{k})-E_c(\vec{k}+\vec{q})+\hbar\omega} \;. \tag{9}$$

Since we are interested only in transitions near the $\Gamma$ point we have taken in Eq. (7) the momentum matrix elements $P_{cv}$ to be independent of $\vec{k}$ and equal to some average value at the $\Gamma$ point.[14]

For the quasiparticle energies $E_c(\vec{k})$ and $E_v(\vec{k})$ appearing in Eq. (9) we write

$$E_c(\vec{k})=\epsilon_{c\vec{k}}+\Sigma_e(\vec{k},E_{c\vec{k}}) \;, \tag{10}$$

$$E_v(\vec{k})=\epsilon_{v\vec{k}}+\Sigma_h(\vec{k},E_{v\vec{k}}) \;, \tag{11}$$

where $\Sigma_e$ and $\Sigma_h$ are the self-energy corrections to the noninteracting single-particle energies $\epsilon_{ck}$ and $\epsilon_{vk}$. We calculate them in the random-phase approximation (RPA) using the plasmon-pole approximation[15,16] for the electron-electron interaction and the polaron $\epsilon_0^*$ approximation[15,16] for the electron-phonon interaction in GaAs. In the latter, the high-frequency dielectric constant $\epsilon_\infty$ is replaced by the static $\epsilon_0$. [For typical range of the $e$-$h$ density $n\sim 10^{16}$ $\mathrm{cm^{-3}}$–$2\times 10^{17}$ $\mathrm{cm^{-3}}$, the plasma frequency $\hbar\omega_p$ (5–24 meV) is much smaller than LO-phonon frequency (36.8 meV), a condition for the validity of $\epsilon_0^*$ approximation.] For electrons, we have[17]

$$\Sigma_e(\vec{k},U)=-\frac{e^2}{2\pi^2\epsilon_0}\int\frac{d^3q}{q^2}\left[f(E_{\vec{k}-\vec{q}})+\omega_p^2\left(\frac{f(E_{\vec{k}-\vec{q}})}{(\epsilon_{\vec{k}-\vec{q}}-U)^2-\omega_q^2}+[2\omega_q(\omega_q+\epsilon_{\vec{k}-\vec{q}}-U)]^{-1}\right)\right] \;, \tag{12}$$

where

$$\omega_q^2=\omega_p^2+aq^2+bq^4 \tag{13}$$

and $a$ and $b$ are parameters giving the plasmon dispersion of the $e$-$h$ system with density $n$. A similar expression holds for heavy holes $[\Sigma_h(\vec{k},U)]$, except here one has to include the coupling between $hh$ and $lh$ bands.[15] The various parameters are taken as[16] $a=\omega_p^2/k_{\mathrm{FT}}^2$; $b=(\hbar/4\mu)^2$, $\mu^{-1}=m_c^{-1}+m_{dh}^{-1}$; $\omega_p^2=4\pi ne^2/(\epsilon_0\mu_0)$, $\mu_0^{-1}=m_c^{-1}+A$ where $m_{dh}$ and $A^{-1}$ are the density-of-state mass and optical mass for the holes, respectively. Also $m_h$, $m_l$, and $m_c$ denote the effective masses for $hh$, $lh$, and conduction bands, respectively. The contribution to screening length $k_{\mathrm{FT}}$ comes from both free electrons in the conduction band and holes in the valence band. An exact expression for $k_{\mathrm{FT}}$ at finite temperatures is given in Ref. 18. However, for the temperature and plasma density range which we consider here, the electrons in the conduction band can be almost considered as degenerate, whereas holes in the valence band are almost nondegenerate. This is because for the range of $T$ and $n$ under consideration, the thermal energy is quite small compared to the electronic Fermi energy and large compared to the hole Fermi energy. In this case $k_{\mathrm{FT}}$ can be written as

$$k_{\mathrm{FT}}^2=4e^2(k_F m_c/\hbar^2+k_F^3/3k_BT)\epsilon_0\pi \;, \tag{14}$$

where $k_B$ is the Boltzman constant. The self-energies $\Sigma_e$ and $\Sigma_h$ can thus be calculated for any $\vec{k}$ and $U$ using various band parameters as listed in Table I.[19] However, their $\vec{k}$ and $U$ dependence is found to be quite weak[8] as expected. In Fig. 2, we have plotted $\Sigma_e(k_F,\epsilon_F)$ and $\Sigma_h(k_F,\epsilon_F)$ as a function of plasma density $n$ for two typical values of plasma temperatures. The temperature effect is also seen to be not very important.

In order to include $e$-$h$ attraction, we have to solve the integral equation (8) for $\chi_{cv}$. In the absence of free carriers, it can be solved exactly[3] and leads to Elliott's result[1] for optical absorption in insulating semiconductors. In the presence of free car-

TABLE I. Band parameters used for GaAs (Ref. 19).

| $m_c$ | $m_l$ | $m_h$ | $m_{dh}$ | $A$ | $\epsilon_0$ |
|---|---|---|---|---|---|
| 0.067 | 0.085 | 0.52 | 0.543 | 7.65 | 12.35 |

riers, the integral equation is difficult to solve analytically. However, one can obtain an approximate solution by using an approximation due to Mahan.[3,7] It makes use of the small phase space involved in $\vec{k}\rightarrow\vec{k}'$ transitions and assumes the factorization of the $e$-$h$ interaction as

$$V_s(\vec{k}-\vec{k}')=\frac{V_s(k,\tilde{k})V_s(k',\tilde{k})}{V_s(\tilde{k},\tilde{k})}\ , \tag{15}$$

where $V_s(k,k')$ is the angular average of $V_s(\vec{k}-\vec{k}')$ and $\tilde{k}$ is related to the incident photon frequency $\omega$ such that

$$E_{c\tilde{k}}-E_{v\tilde{k}}=\hbar\omega\ . \tag{16}$$

In this approximation, for $q\rightarrow 0$, Eq. (8) leads to

$$\epsilon_2^b(\omega)=C\sum_{\vec{k}}[f_v(E_{\vec{k}})-f_c(E_{\vec{k}})]\pi\delta(E_{v\vec{k}}-E_{c\vec{k}}+\hbar\omega)[|1-Y(\omega)|]^{-2}$$
$$\times\{[1-Y_1(\omega)+\Delta(k,\tilde{k})X_1(\omega)]^2-Y_2(\omega)[\Delta(k,\tilde{k})X_2(\omega)-Y_2(\omega)]\}\ , \tag{17}$$

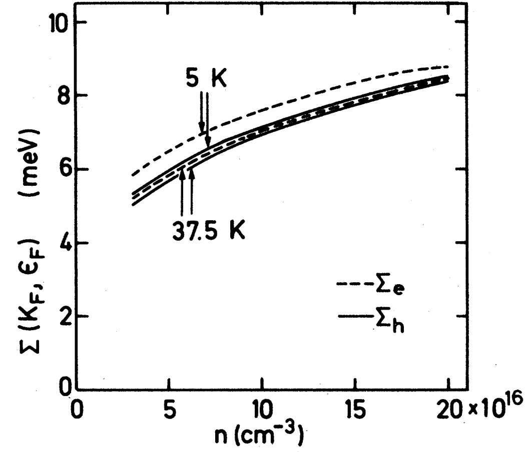

FIG. 2. Real part of self-energies $\Sigma(k_F,\epsilon_F)$ for electrons and holes of $e$-$h$ plasma in GaAs as a function of plasma density $n$ and for two temperatures.

where $\Delta(k,\tilde{k})=V_s(k,\tilde{k})/V_s(\tilde{k},\tilde{k})$ and subscripts 1 and 2 denote, respectively, the real and imaginary part of $X(\omega)$ and $Y(\omega)$ which are defined as

$$X(\omega)=-\frac{1}{2}\sum_{\vec{k}}V_s(k,\tilde{k})\chi^0_{cv}(\vec{k},\omega-i\delta)\ , \tag{18}$$

$$Y(\omega)=-\frac{1}{2}\sum_{\vec{k}}[|V_s(k,\tilde{k})|^2/V_s(\tilde{k},\tilde{k})]\chi^0_{cv}(\vec{k},\omega-i\delta)\ . \tag{19}$$

Equation (17) which is quite general, can be simplified further if one considers the effective-mass approximation for valence and conduction bands and takes the self-energies to be constant thus neglecting the relatively weak $k$ and energy dependence. In this approximation, $\tilde{k}$ can be written as [Eq. (16)]

$$\hbar\omega=\tilde{E}_g+\hbar^2\tilde{k}^2/2m_{cv};\quad m_{cv}^{-1}=m_c^{-1}+m_h^{-1}\ , \tag{20}$$

$$\tilde{E}_g=E_g+\Sigma_e+\Sigma_h\ , \tag{21}$$

where $E_g$ is the experimental band gap for intrinsic GaAs. One can also show that within this approximation $\Delta(k,\tilde{k})\approx 1$ and $Y_2(\omega)=X_2(\omega)$. Thus Eq. (17) reduces to a simplified form

$$\epsilon_2^b(\omega)=\epsilon_2^a(\omega)R(\omega)\ , \tag{22}$$

where

$$\epsilon_2^a(\omega)=C\sum_{\vec{k}}[f_v(E_{\vec{k}})-f_c(E_{\vec{k}})]\pi\delta(E_{v\vec{k}}-E_{c\vec{k}}+\hbar\omega) \tag{23}$$

is the dielectric function without including $e$-$h$ interaction but retaining the self-energy correction for electrons and holes and

$$R(\omega)=\left|\frac{1-Y_1(\omega)+X_1(\omega)}{1-Y(\omega)}\right|^2 \tag{24}$$

gives the excitonic enhancement due to $e$-$h$ interaction. A discussion of the influence of the $e$-$h$ interaction based on Eq. (22) has previously been given by Zimmermann[7] for the $e$-$h$ plasma in the parabolic band approximation. However, our result [Eq. (17)] is quite general and includes the self-energy corrections, which we consider as being crucial for internal consistency in the perturbation treatment. Moreover, because of renormalization of the threshold, these corrections are necessary for comparing theoretical and experimental line shapes. Haug and Thoai[9] have also studied independently these many-particle effects on the gain line shapes making use of similar approximations.

For completeness, we also give an expression for the imaginary part of the dielectric function $\epsilon_2^c(\omega)$ calculated by neglecting the $\vec{k}$-selection rule for optical transitions as[14]

$$\epsilon_2^c(\omega)=C'\int_0^{(\hbar\omega-\tilde{E}_g)} d\epsilon\,\epsilon^{1/2}(\hbar\omega-\tilde{E}_g-\epsilon)^{1/2} \times[f_v(\hbar\omega-\tilde{E}_g-\epsilon)-f_c(\epsilon)]d\epsilon\ , \qquad (25)$$

where $C'$ is a constant depending on the band parameters. Thus knowing $\epsilon_2(\omega)$ [Eqs. (22), (23), and (25)] one can calculate the absorption coefficient from the relation

$$\alpha(\omega)=[\omega/\eta(\omega)c]\epsilon_2(\omega)\ , \qquad (26)$$

where $\eta(\omega)$ is the refractive index for the crystal.

## III. RESULTS AND DISCUSSION

On the basis of Eq. (22) the absorption and emission line shapes including many-body effects are calculated. Results for GaAs are plotted in Fig. 3 for a typical plasma density and temperature. Theoretical line shapes in the single-particle model, neglecting $e$-$h$ interaction, with (curve a) and without (curve c) $\vec{k}$-selection rule are also displayed for comparison. Electron-hole interaction gives rise to an excitonic enhancement in $\alpha_b(\omega)$ compared to $\alpha_a(\omega)$ which is most prominent near the crossover, while for higher energies $\alpha_b(\omega)$ approaches $\alpha_a(\omega)$. The line shape in the non-$\vec{k}$-conserving model (curve c) is similar to that obtained by including $e$-$h$ interaction in the gain region but it becomes completely different in the absorption region far above the crossover where it goes approximately as $(\hbar\omega-E_g)^2$.

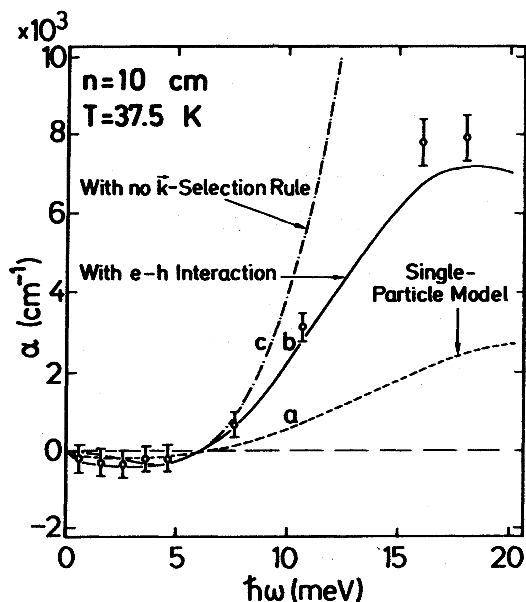


FIG. 3. Absorption coefficient as a function of photon energy measured with respect to the effective gap $\tilde{E}_g=1.5054$ eV (Ref. 20). Values of $\alpha(\omega)$ for curves a and b and for experimental points are in absolute units. [In the limit of large $\hbar\omega$ the experimental points have been normalized to those reported in M. D. Sturge, Phys. Rev. 127, 768 (1962).] However, $\alpha(\omega)$ for curve c is in arbitrary units.

Comparison with the experimental data only in the gain region does not seem to be sufficient for drawing any conclusion about the validity of a theoretical concept. This is due to the fact that in this region, the line shapes are quite sensitive to the plasma temperature which is usually not known accurately.[10,11] Furthermore, here the uncertainties in the measured intersities are relatively large.[10] Theoretical gain line shapes in either of these models are also not very different at high temperatures (in Refs. 10 and 11, line shapes were fitted with non-$\vec{k}$-conserving model in the gain region only). Thus to draw any definite conclusion, one must compare the absorption line shapes above the crossover ($\hbar\omega>E_g$). Figure 3[20] clearly shows that the experimental results agree well with curve b obtained by including many-body effects. The agreement is good not only in terms of the shape of the absorption and gain lines but also for the absolute magnitude. However, a small discrepancy of 3 meV still remains in the experimental and theoretical onset ($\tilde{E}_g$) of the gain.[21] In contrast to this, curves a and c are far from agreement with experimental line shapes.

In Figs. (4a)–(4d) we have displayed theoretical line shapes calculated from Eq. (22) for plasma density ranging from $3\times10^{16}$ cm$^{-3}$ to $2\times10^{17}$ cm$^{-3}$ and temperature ranging from 5 to 100 K. In all these calculations, many-body effects are found to be quite important in determining the line shapes. Excitonic enhancement which strongly changes the line shapes near the crossover, persists even quite far from the absorption edge. However, its effect reduces with increase in plasma density because of large screening to $e$-$h$ interactions. The effect of temperature on the line shapes is more important within the energy range of a few $kT$ around the crossover. Higher temperature reduces the gain region, and for sufficiently large temperatures, the gain region almost disappears [Figs. 4(c)–4(d)].

Experimentally the temperature and concentration of the highly excited $e$-$h$ plasma are not known exactly and it is of great interest to know them accurately. For instance, in the experimental studies[10] of the relaxation of the hot $e$-$h$ plasma, one creates electrons and holes with large excitation energies by a picosecond laser pulse. The hot electrons and holes start cooling to the lattice temperature. (Note that the relaxation time of $e$-$h$ plasma in direct-gap semi-

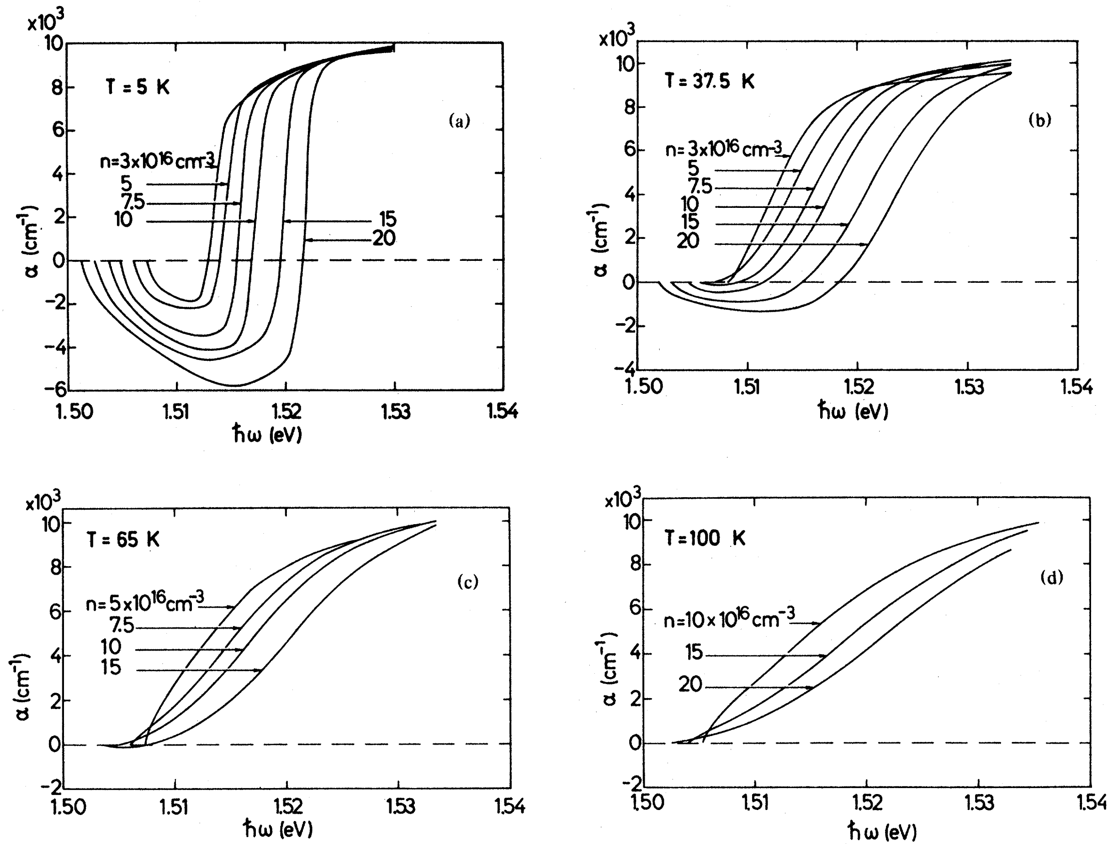


FIG. 4. (a)–(d) Absorption coefficient $\alpha(\omega)$ as a function of photon energy for different values of plasma density $n$ and temperature $T$.

conductors is of the order of several hundred picoseconds whereas the electrons and holes attain equilibrium among themselves very fast. Thus one can define a temperature for the $e$-$h$ plasma.) The temperature evolution of the $e$-$h$ plasma is then studied indirectly by measuring the absorption and gain line shapes by another picosecond pulse at later times from the excitation pulse. As we have seen the absorption and emission line shapes strongly depend on the plasma $n$ and $T$. The comparison of the experimental line shapes with those obtained theoretically including many-body effects from Eq. (22) can be used to extract $n$ and $T$ accurately. This procedure has been used in fact in Ref. 10 for studying the temperature evolution of $e$-$h$ plasma in GaAs. However, in this work, the experimental line shapes are compared with those obtained theoretically by neglecting $\vec{k}$-selection rule [Eq. (25)] which are wrong as we have discussed earlier. Recently this method has also been used[22] for extracting plasma $T$ and $n$ in germanium by comparing the experimental and theoretical [obtained from Eq. (22) with some modifications] absorption line shapes for the direct optical transitions.

In conclusion, the many-body effects are very important in calculating the absorption and emission line shapes from $e$-$h$ plasma in direct-gap semiconductors. The line shapes are sensitive on plasma $n$ and $T$ in a wide energy range and thus can be used to extract these parameters more accurately than in the method of luminescence. This is because the luminescence line shapes are not sensitive to plasma density and therefore are good only for determining temperature.

## ACKNOWLEDGMENT

We would like to thank Professor T. M. Rice for several discussions and a critical reading of the manuscript.

[1]R. J. Elliott, Phys. Rev. 108, 1384 (1957).
[2]W. Hanke and L. J. Sham, Phys. Rev. B 12, 4501 (1975); Phys. Rev. Lett. 43, 387 (1979); Phys. Rev. B 21, 4656 (1980).
[3]G. D. Mahan, Phys. Rev. 153, 882 (1967).
[4]V. M. Asnin and A. A. Rogachev, Phys. Status Solidi 20, 755 (1967); V. M. Asnin, G. L. Eristavi, and A. A. Rogachev, *ibid.* 29, 443 (1968).
[5]E. A. Meneses and R. Luzzi, Solid State Commun. 12, 447 (1973).
[6]B. F. Brinkman and P. A. Lee, Phys. Rev. Lett. 31, 237 (1973).
[7]R. Zimmermann, Phys. Status Solidi B 86, K63 (1978).
[8]K. Arya and W. Hanke, Solid State Commun. 33, 739 (1980).
[9]H. Haug and D. B. Thoai (unpublished).
[10]D. Von der Linde and R. Lambrich, in *Picosecond Phenomena*, edited by C. V. Shank, I. P. Ippen, S. L. Shapiro (Springer-Verlag, New York, 1978), Vol. 4; also see, Phys. Rev. Lett. 42, 1090 (1979).
[11]O. Hilderbrand, E. O. Goebel, K. M. Romanek, H. Weber, and G. Mahler, Phys. Rev. B 17, 4775 (1978).
[12]J. Shah, R. F. Lehery, and W. Wiegemann, Phys. Rev. B 16, 1577 (1977).
[13]D. Von der Linde and R. Lambrich (unpublished).
[14]G. Lasher and F. Stern, Phys. Rev. 133, A553 (1964).
[15]T. M. Rice, Nuovo Cimento B 33, 226 (1974); G. Beni and T. M. Rice, Phys. Rev. Lett. 37, 874 (1976).
[16]M. Rösler and R. Zimmermann, Phys. Status Solidi B 83, 85 (1977).
[17]We include only the real part of the self-energies $\Sigma_e$ and $\Sigma_h$ in our calculations. The imaginary part is responsible for a tail below the effective gap and causes small changes in the line shape near the onset of the gain.
[18]R. Zimmermann and M. Rösler, Phys. Status Solidi B 75, 633 (1976).
[19]G. Beni and T. M. Rice, Phys. Rev. B 18, 768 (1978).
[20]$\tilde{E}_g$ is calculated from Eq. (21) by including a contribution of the 0.4 meV due to multiple scattering (see Ref. 19). This still leaves a discrepancy of 3 meV in the experimental and theoretical onset of the gain; the theoretical onset in Fig. 3 is adjusted by this amount to give empirical agreement.
[21]This discrepancy may be due to the fact that we calculate $\tilde{E}_g$ using plasma $n = 10^{17}$ cm$^{-3}$ and $T = 37.5$ K as quoted in Ref. 10. However, in this reference, $n$ and $T$ were obtained by fitting the experimental gain line shapes with those obtained by neglecting the $\vec{k}$-selection rule (curve c), which is not correct, as discussed in the text.
[22]H. Schweizer, A. Forchel, and K. Arya (unpublished).